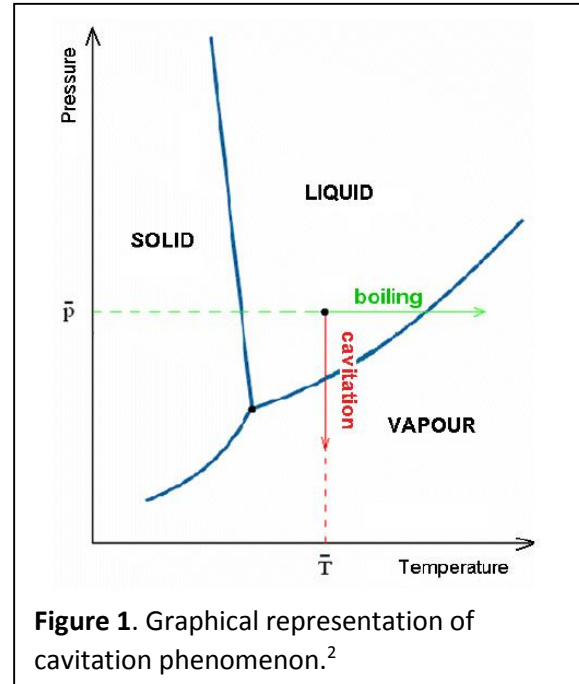


ABOUT THE COMPANY

Mechanical Solutions, Inc. (MSI) is an engineering firm headquartered in Whippany, NJ, which specializes in mechanical engineering design, testing and analysis, and also provides services in fluid machinery design and computational fluid dynamics (CFD) analysis.

INTRODUCTION

Cavitation is a thermodynamically non-reversible process defined as the formation and subsequent collapse of vapor bubbles caused by the drop in pressure in the fluid domain, as illustrated in **Figure 1**. The collapse of these bubbles can produce a shock wave strong enough to damage machine parts, and as such, cavitation is usually an undesirable phenomenon. It can also generate significant vibration and noise, cause rotordynamic instabilities and blade erosion, and negatively affect general machinery performance.



CHARACTERIZATION

Cavitation in turbomachinery is usually predictable, and can be characterized by two numbers. The first one is Net Positive Suction Head (NPSH), which expresses the cavitation requirements in terms of head:

$$NPSH = \frac{p_{t1} - p_{vapor}}{\rho_L g}$$

The other is the cavitation coefficient, which is a dimensionless number used in modelling and experimental results:

$$\sigma = \frac{p_{t1} - p_{vapor}}{0.5 \rho_L v^2}$$

In those equations, p_{t1} stands for inlet or exit total pressure (depending on whether the machine in question is a pump or a turbine), p_{vapor} stands for vapor pressure of fluid at a given temperature, ρ_L is the liquid density, and v is relative velocity.

Using NPSH, a minimum satisfactory performance can be established for a given machine, called the required NPSH (or NPSHr), usually given by the manufacturer. In practice, NPSHr is often set at 3% below regular output. Then the available NPSH (or NPSHa) can be compared against NPSHr, and if $NPSHa < NPSHr$, then cavitation has reached an undesirable threshold. The NPSH criterion can also be presented as a curve, as shown in **Figure 2**.

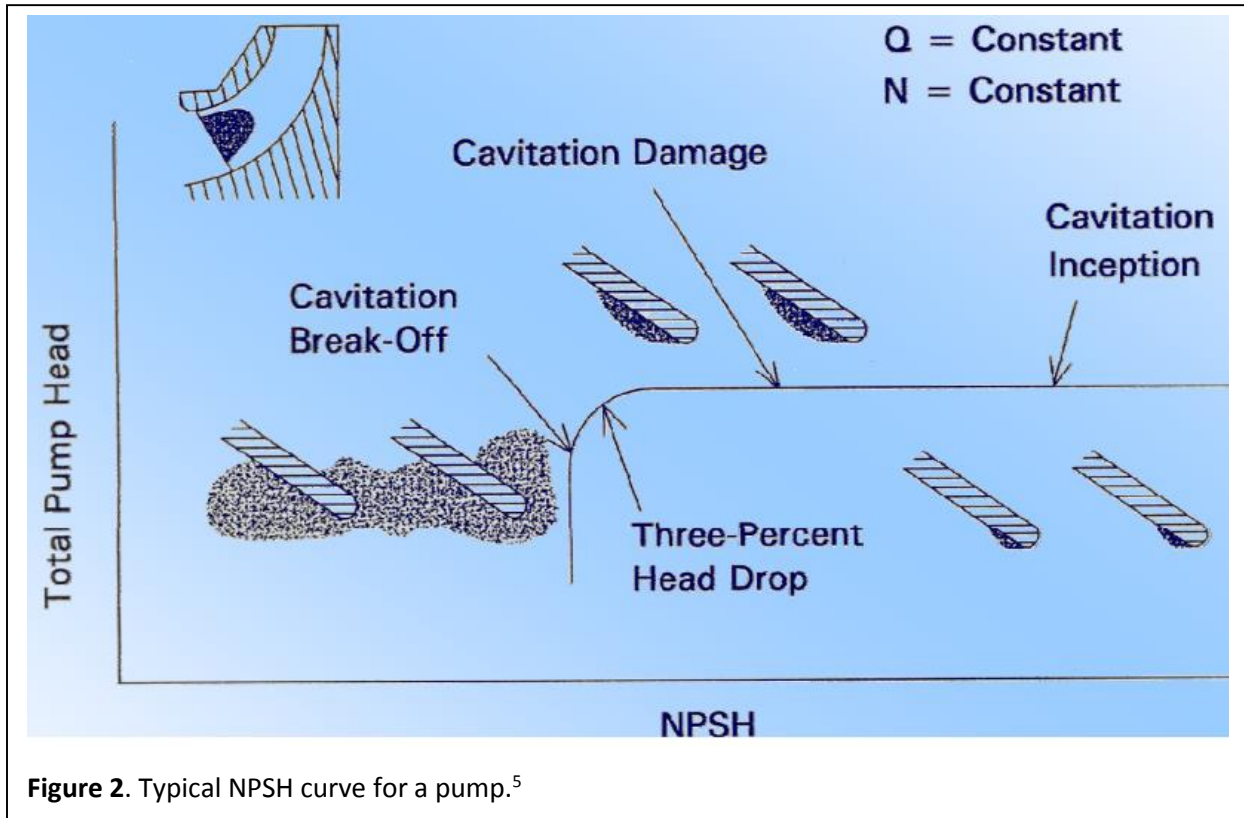


Figure 2. Typical NPSH curve for a pump.⁵

Cavitation can also be worsened by the presence of entrained or dissolved gases in the liquid. These gases would come out of the solution when the pressure drops low enough, and can produce more negative impact on machinery performance, in addition to regular cavitation. This tendency is illustrated in **Figure 3**.

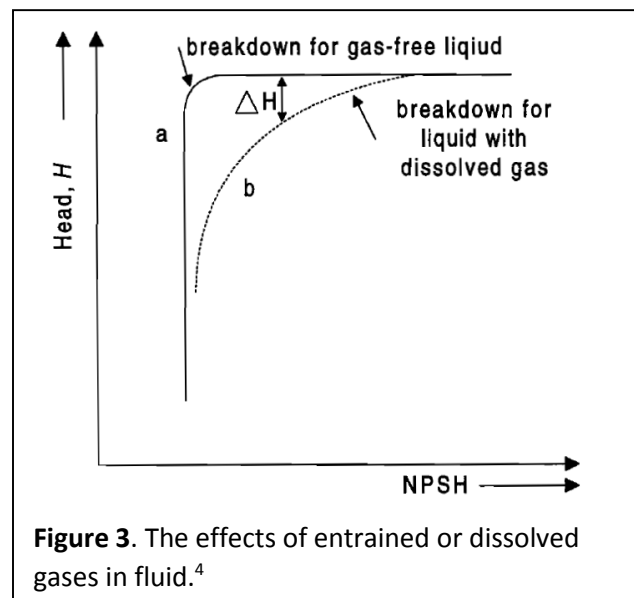


Figure 3. The effects of entrained or dissolved gases in fluid.⁴

Cavitation is also an inherently unstable and unsteady phenomenon. As the vapor cavity grows, it can cause transient effects to occur, such as stall and auto-oscillation, as well as rotordynamic instabilities. These effects can have a profound negative impact on the operation and mechanical integrity of hydraulic turbomachinery, as depicted in **Figure 4**.

Aside from performance issues, cavitation also has a direct impact on machinery parts, through both erosion and corrosion. Cavitation erosion occurs when bubble collapse produces a shock wave near the surface of a part. As the shock wave impacts the surface, it can induce deformation and pitting. Over time, a significant amount of material loss can occur as a result. Furthermore, the shock wave can also work-harden metal parts, making the surface brittle and flaky. Eventually, the entire part may become work-hardened and brittle, leading to structural breakdown, as shown in **Figure 5**.

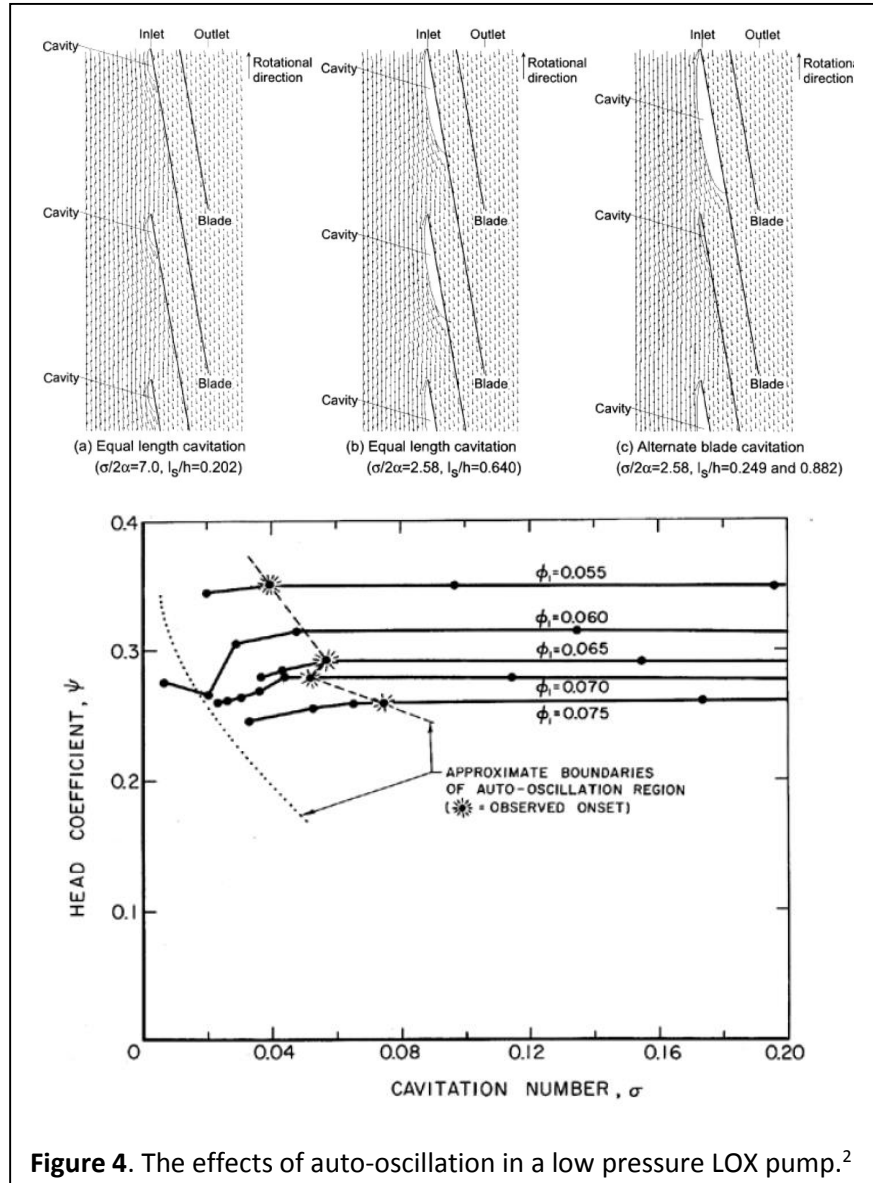


Figure 4. The effects of auto-oscillation in a low pressure LOX pump.²

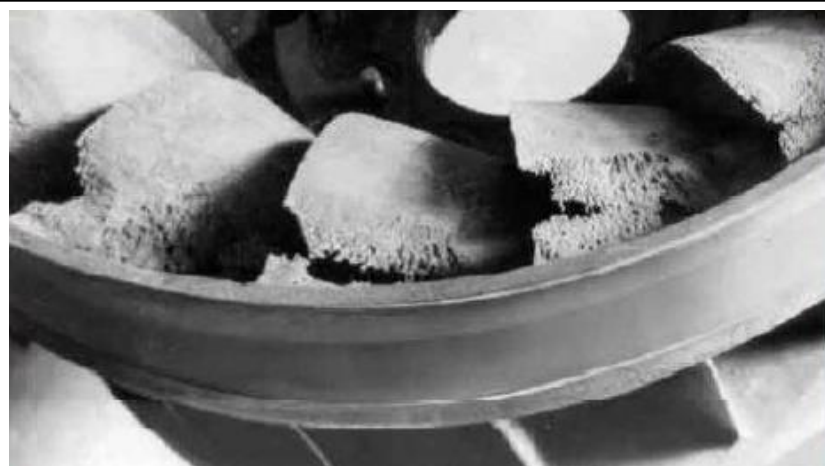


Figure 5. Cavitation damage in a Francis turbine runner.³

AXIAL INDUCER TEST CASE

To postpone the onset of cavitation in pumps, axial inducers are often used to boost inlet pressure, thus increasing NPSH and improving cavitation performance. The inducers are often included in high-energy density industrial pumps, rocket turbopumps, liquid natural gas (LNG) pumps and fire suppression pumps. Moreover, inducers can operate at lower levels of NPSH since their power level is only a fraction of the main impeller, and the much larger throat area of the inducer allows for lower inlet velocities and can swallow more vapor to avoid blockage, as shown in **Figure 6**.

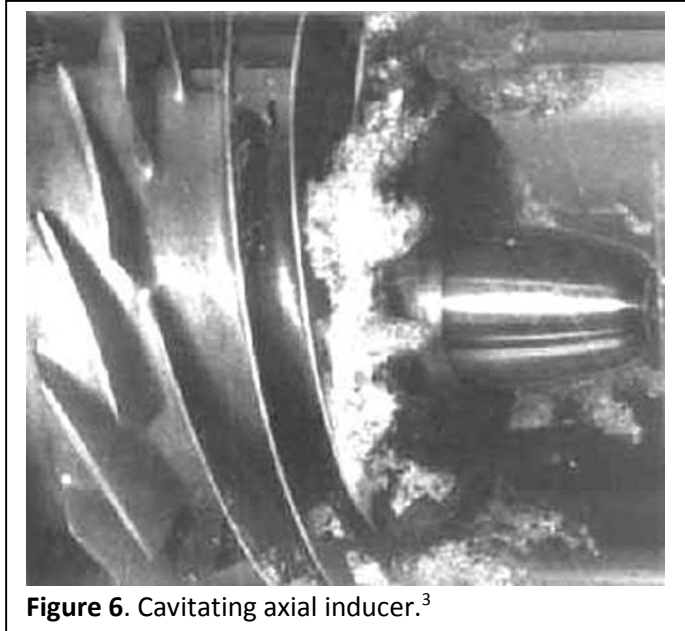


Figure 6. Cavitating axial inducer.³

An axial inducer test case, based on NASA FASTRAC LOX inducer, was created using CFTurbo design software, as presented in **Figure 7**. It employed two radial element vanes with a wrap angle of 349.5 degrees. The meridional flow coefficient was set at 0.1, and the inlet hub to tip ratio at 0.3. At the target flow of $0.014 \text{ m}^3/\text{s}$ and 5000 rpm, the NPSHr of this inducer was set at 1.08 meters.

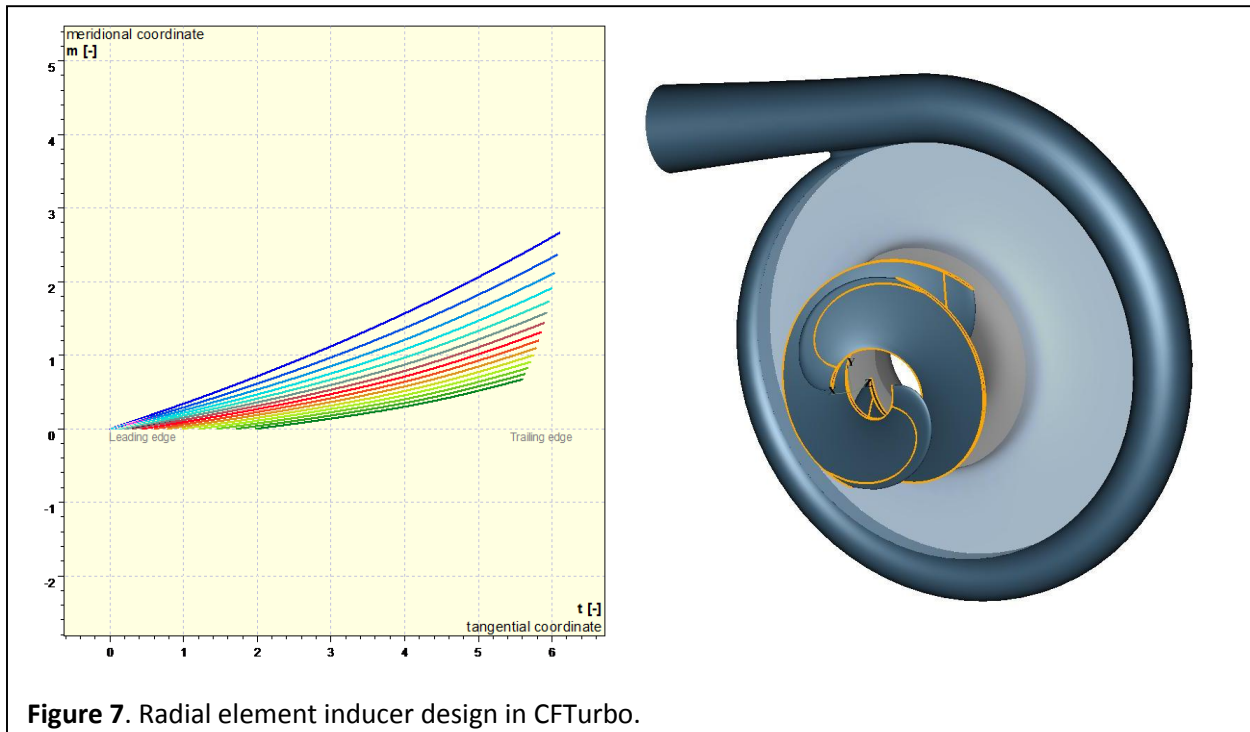


Figure 7. Radial element inducer design in CFTurbo.

The design's performance was then assessed in STAR-CCM+, where it was modeled in the same configuration as the rig test. That model and its mesh are shown in **Figure 8**.

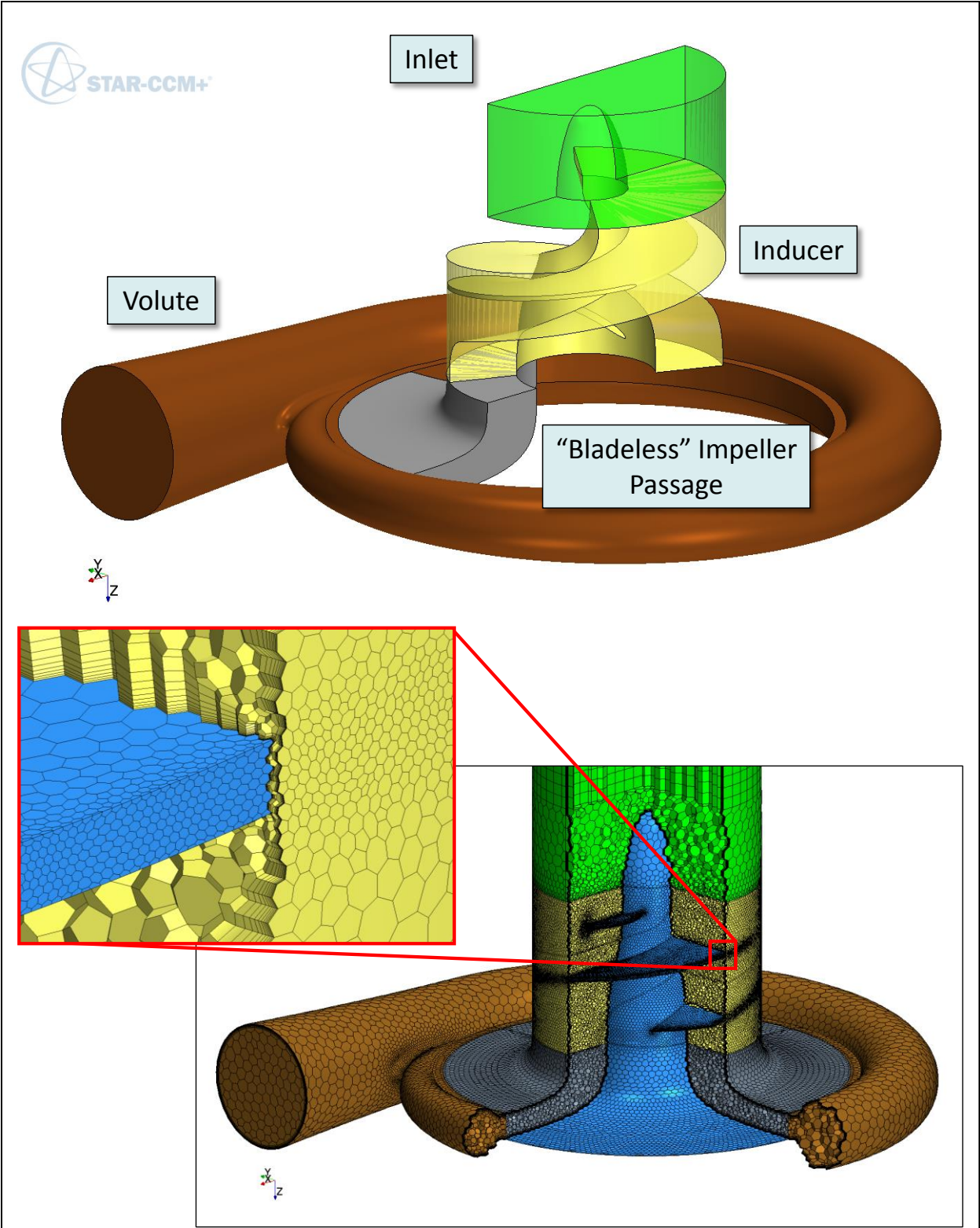
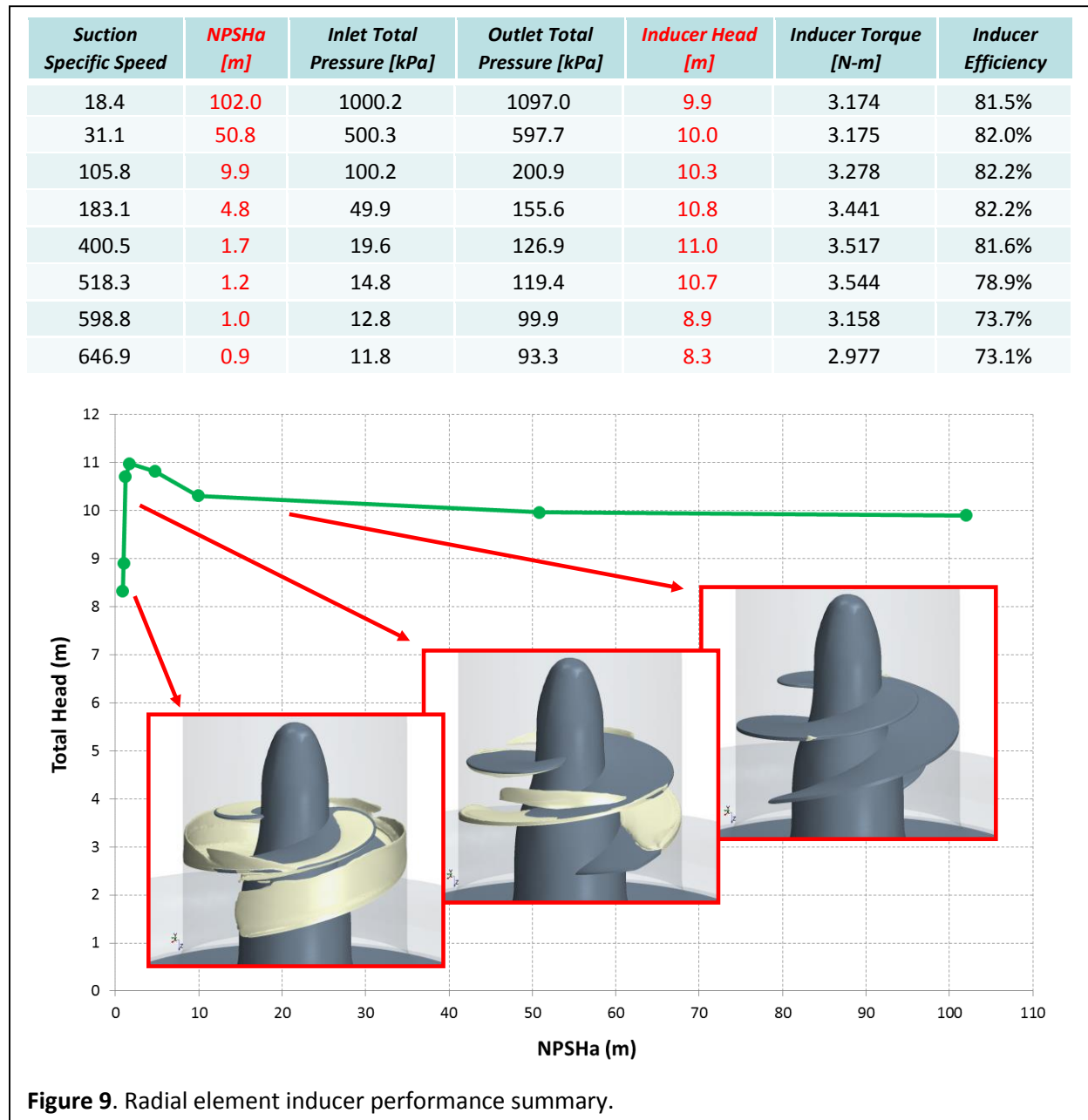


Figure 8. The inducer rig geometry and mesh in STAR-CCM+.

The CFD analysis of the axial inducer was performed using the Shear-Stress Transport (SST) $k-\omega$ turbulence model with curvature correction, which is an industry standard. Pressure and velocity were modeled with 2nd-order segregated flow solver in a transient manner, with a timestep that corresponded to one degree of inducer rotation, and 1e-4 limit for residual convergence of inner iterations. Cavitation was modeled using the Volume of Fluid (VOF) 2nd-order multiphase model, where water and vapor were assumed to be constant-density fluids at 298.15 K. The total pressure at the inlet was sequentially lowered to plot the NPSH curve, and each point on the curve was simulated until all plots for monitored values (pressure, torque, etc.) were judged to have settled, which necessitated more than 30 revolutions for the highly-cavitating cases. The analysis results are presented in **Figure 9**.



The CFD analyses produced an NPSH curve of expected shape, with a breakdown occurring shortly before the NPSHa of 1 m. It is thus evident that this inducer design provides very little safety margin with respect to cavitation. Furthermore, the shape of the NPSH curve, with a “hump” before the breakdown, indicates a possible instability, some of which are listed in **Figure 10**.

Instability type	Frequency range
<i>Surge</i>	System dependant, 3-10 Hz in compressors
<i>Auto-oscillation</i>	System dependant, 0.1-0.4 Ω
<i>Rotating stall</i>	0.5-0.7 Ω
<i>Vaneless diffuser stall</i>	0.05-0.25 Ω
<i>Rotating cavitation</i>	1.1-1.2 Ω
<i>Partial cavitation oscillation</i>	< Ω
<i>Excessive radial force</i>	Some fraction of Ω
<i>Rotordynamic vibration</i>	Some fraction of Ω when critical speed is approached
<i>Blade flutter</i>	Natural frequency of blade in liquid
<i>Cavitation noise</i>	1-20 kHz

Figure 10. Typical Pump Cavitation Instability Frequencies.²

To investigate further, an FFT analysis of the pressure field was performed. Pressure probes were inserted into the fluid domain near the shroud of the inducer, close to the leading edge of the vanes, as illustrated in **Figure 11**. Static pressure was then queried at these locations at every timestep, and the traces subjected to an FFT analysis, presented in **Figure 12** on the next page. It revealed a peak at a known cavitation instability mode known as auto-oscillation, which should be avoided in operation. It is thus desirable to either operate at higher NPSH values to avoid possible performance issues, or develop an alternate inducer design.

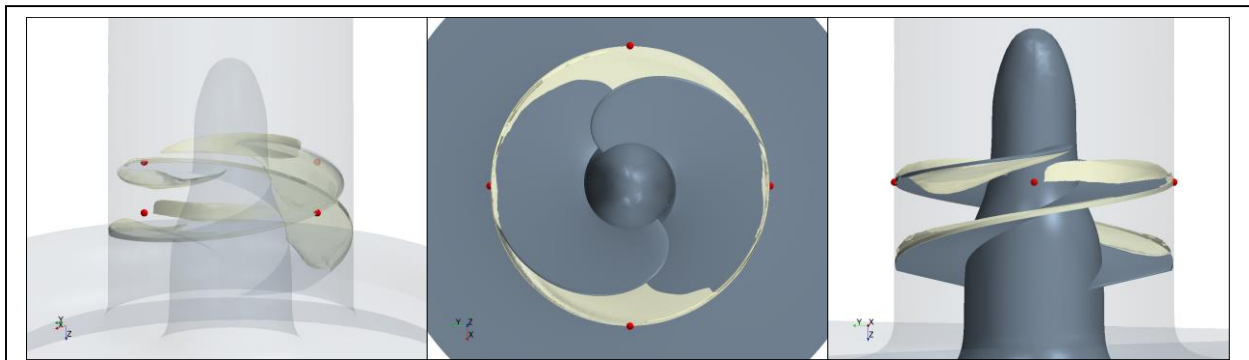


Figure 11. Pressure probe locations in the inducer CFD model.

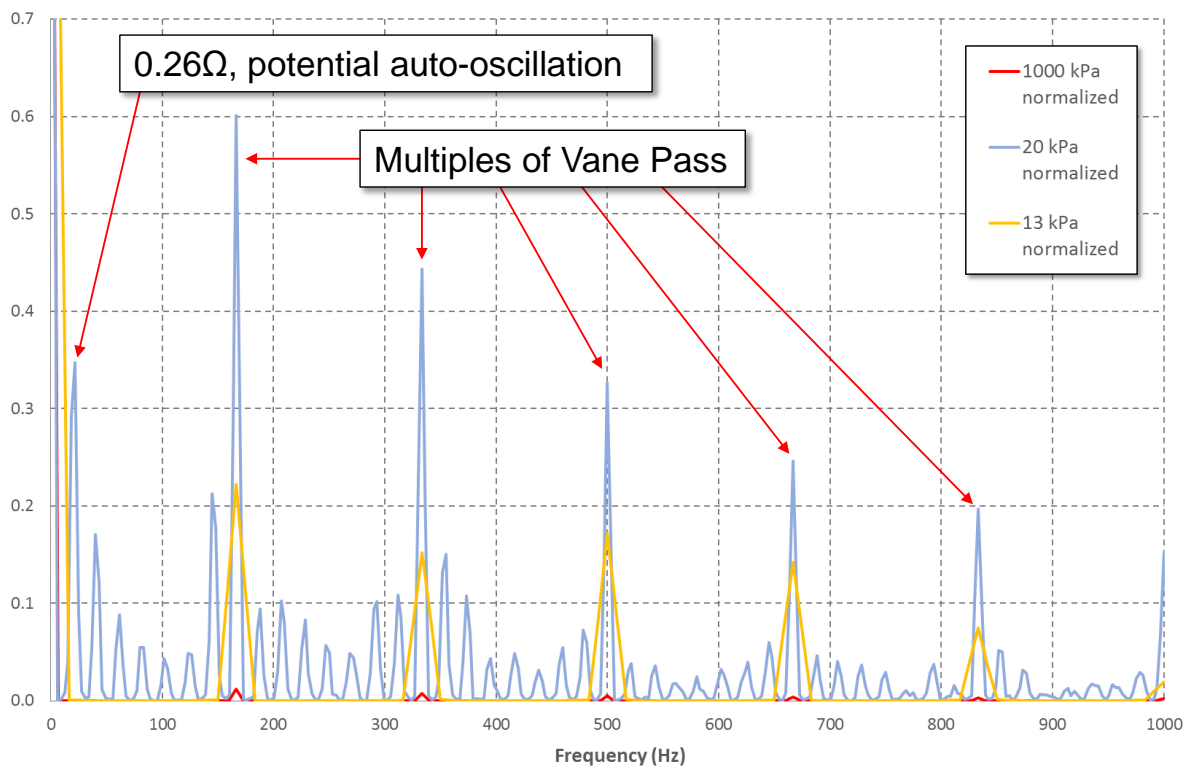
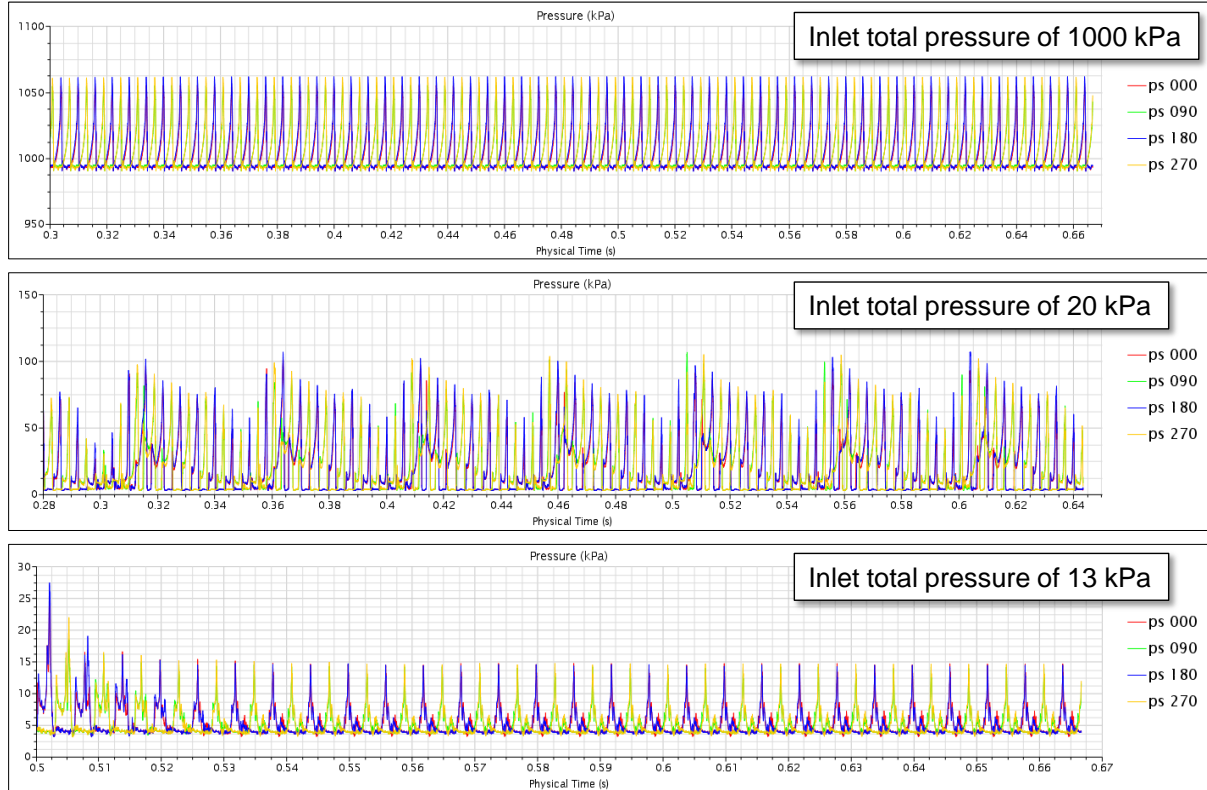


Figure 12. Summary of the cavitation FFT analysis.

Consequently, another design was created using CFTurbo to increase the safety margin, as presented in **Figure 13**. The design was switched from radial element vanes to helical vanes with a cant of 10 degrees, and it employed 4 vanes instead of two, to reduce the vane loading that can lead to instabilities at lower values of NPSH. Inlet hub to tip ratio was maintained at 0.3, but the meridional flow coefficient was lowered to 0.085, and the hub wrap angle was raised to 374.3 degrees. The alternate design was then subjected to the same analyses as the radial element design in STAR-CCM+.

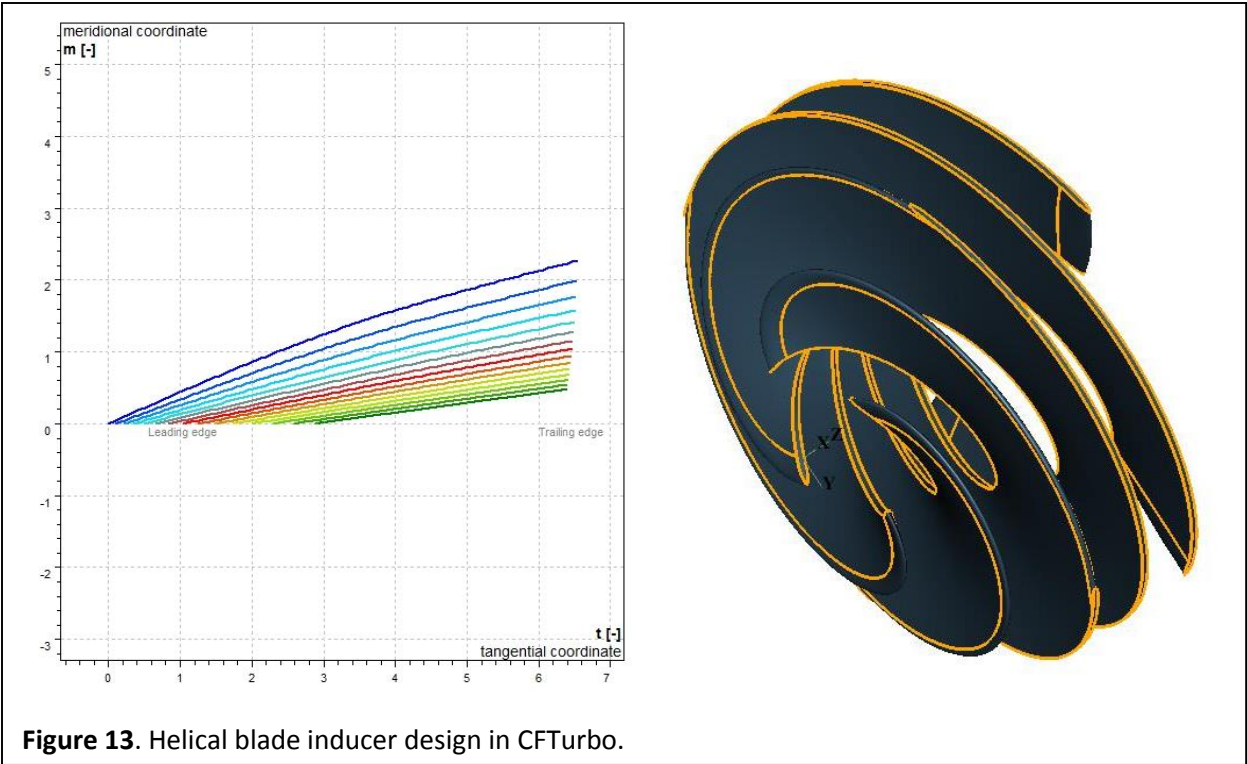


Figure 13. Helical blade inducer design in CFTurbo.

From the NPSH curve shown in **Figure 14**, it is evident that the alternate design has a much higher safety margin with respect to NPSH_r, as it has not yet begun to lose head at 1.08 meters of NPSH_a, and does not present a “hump” before the breakdown is initiated.

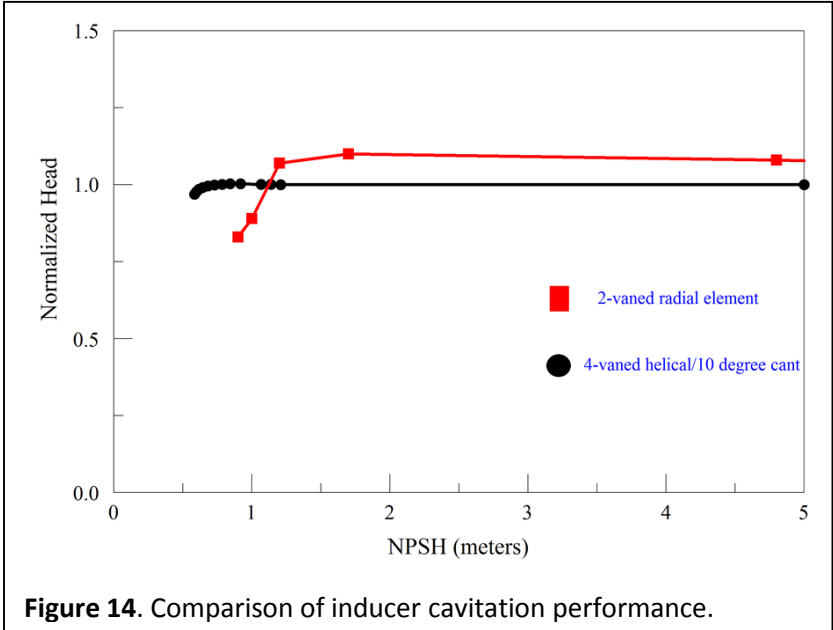


Figure 14. Comparison of inducer cavitation performance.

CONCLUSIONS

Transient multiphase CFD analysis can be successfully applied to turbopumps flows with cavitation to determine the suitability of prototype designs to a particular NPSHr. Furthermore, it can detect potentially unstable cavitation modes, thus helping increase safety and reduce costs in development.

REFERENCES

1. Bennett, E., "Advanced Methodology for Low NPSH Axial Pump Inducers", ASME Fluids Engineering Division Summer Meeting, 2009.
2. Bramanti, C., "Experimental Study of Cavitation and Flow Instabilities in Space Rocket Turbopumps and Hydrofoils", University of Pisa Doctoral Dissertation, 2005.
3. Brennen, C., "Hydrodynamics of Pumps", Oxford Press, 1994.
4. Wood, D., et al, "Application Guidelines for Pumping Liquids That Have a Large Dissolved Gas Content", 15th Texas A&M Pump Symposium, 1998.
5. Visser, F., "Cavitation in Centrifugal Pumps and Prediction Thereof", Tutorial, 2005 ASME Fluids Engineering Division Summer Conference, 2005.